Dalton Transactions

ROYAL SOCIETY OF CHEMISTRY

PAPER

View Article Online
View Journal | View Issue

Cite this: *Dalton Trans.*, 2023, **52**, 13216

Molecular hydrogen and water activation by transition metal frustrated Lewis pairs containing ruthenium or osmium components: catalytic hydrogenation assays†

Sophie Beard, Alejandro Grasa, Fernando Viguri, Ricardo Rodríguez, José A. López, Fernando J. Lahoz, Pilar García-Orduña, Pilar Lamata * and Daniel Carmona *

The transition metal frustrated Lewis pair compounds [(Cym)M(κ^3S,P,N-**HL1**)][SbF_6] (Cym = η^6-*p*-MeC_6H_4iPr; **H_2L1** = *N*-(*p*-tolyl)-*N*′-(2-diphenylphosphanoethyl)thiourea; M = Ru (**5**), Os (**6**)) have been prepared from the corresponding dimer [{(Cym)MCl}$_2$(μ-Cl)$_2$] and **H_2L1** by successive chloride abstraction with $NaSbF_6$ and $AgSbF_6$ and NH deprotonation with $NaHCO_3$. Complexes **5** and **6** and the previously reported phosphano–guanidino compounds [(Cym)M(κ^3P,N,N′-**HL2**)][SbF_6] [**H_2L2** = *N*,*N*′-bis(*p*-tolyl)-*N*″-(2-diphenylphosphanoethyl) guanidine; M = Ru (**7**), Os (**8**)] and pyridinyl–guanidino compounds [(Cym)M(κ^3N,N′,N″-**HL3**)][SbF_6] [**H_2L3** = *N*,*N*′-bis(*p*-tolyl)-*N*″-(2-pyridinylmethyl) guanidine; M = Ru (**9**), Os (**10**)] heterolytically activate H_2 in a reversible manner affording the hydrido complexes [(Cym)MH(**H_2L**)][SbF_6] (**H_2L** = **H_2L1**; M = Ru (**11**), Os (**12**); **H_2L** = **H_2L2**; M = Ru (**13**), Os (**14**); **H_2L** = **H_2L3**; M = Ru (**15**), Os (**16**)). DFT calculations carried out on the hydrogenation of complex **7** support an FLP mechanism for the process. Heating **9** and **10** in methanol yields the orthometalated complexes [(Cym)M(κ^3N,N′,C-**H_2L3**$_{-H}$)][SbF_6] (M = Ru (**17**), Os (**18**)). The phosphano–guanidino complex **7** activates deuterated water in a reversible fashion, resulting in the gradual deuteration of the three cymene methyl protons through sequential C(sp^3)–H bond activation. From DFT calculations, a metal–ligand cooperative reversible mechanism that involves the O–H bond activation and the formation of an intermediate methylene cyclohexenyl complex has been proposed. Complexes **5–10** catalyse the hydrogenation of the C=C double bond of styrene and a range of acrylates, the C=O bond of acetophenone and the C=N bond of *N*-benzylideneaniline and quinoline. The C=C double bond of methyl acrylate adds to catalyst **9**, affording complex **19** in which a new ligand exhibiting a *fac* κ^3N,N′,C coordination mode has been incorporated.

Received 22nd July 2023,
Accepted 24th August 2023

DOI: 10.1039/d3dt02339g

rsc.li/dalton

Introduction

There are known examples of intra- and intermolecular combinations of Lewis acids and bases that in solution do not form the corresponding adducts usually due to steric hindrance. These acid–base couples are referred to as frustrated Lewis pairs (FLP). The first examples of FLP systems were based on representative elements, boron for the acidic centre and phosphorus or nitrogen for the basic centre. A milestone in the development of such systems was the discovery in 2006 by Stephan and co-workers that such species were capable of activating reversibly and heterolytically the hydrogen molecule under mild conditions.[1] Shortly after, it was found that FLP species could activate many other small (CO_2, CO, SO_2, N_2O, NO) and organic (olefins, alkynes) molecules in a concerted and cooperative manner, following new reaction pathways.[2]

Much less developed, but becoming increasingly important, are FLPs in which one of the components is a transition metal fragment. They are called transition metal frustrated Lewis pairs (TMFLPs). Introducing a transition metal into the system gives the FLP, on the one hand, greater structural diversity

Departamento de Catálisis y Procesos Catalíticos. Instituto de Síntesis Química y Catálisis Homogénea (ISQCH), CSIC – Universidad de Zaragoza, Pedro Cerbuna 12, 50009 Zaragoza, Spain. E-mail: dcarmona@unizar.es, plamata@unizar.es

†Electronic supplementary information (ESI) available: Preparation and characterization of **H_2L1** and complexes **1–4**. Kinetic studies for the H/D exchange of complex **7**. NMR and DFT studies on the fluxionality of the complexes **5**, **6**, **11** and **12**. NMR spectra of compounds **H_2L1**, **1–6** and **11–19**. Crystallographic data of complexes **2**, **4–6**, **13**, **14**, **17** and **19**. DFT calculations for the hydrogenation reaction and the H/D exchange process. CCDC 2240240, 2240241, 2240243–2240248. For ESI and crystallographic data in CIF or other electronic format see DOI: **https://doi.org/10.1039/d3dt02339g**

and, on the other hand, access to fundamental reactions of transition metal compounds which are characteristic of homogeneous catalysis.[3]

An important feature of some FLP systems is that they can show their activity even if the classical Lewis acid–base adduct is stable, provided that the dissociated form is thermally accessible. Such a type of FLP is denominated as a masked FLP.[4] In this regard, we have recently reported the preparation of masked TMFLPs based on the phosphano–guanidine **H_2L2** and pyridinyl–guanidine **H_2L3** ligands depicted in Scheme 1.[5] These are half-sandwich (ring) M-complexes (**A**, **B** in Scheme 1) with deprotonated monoanionic **HL2** or **HL3** species acting as the κ^3 ligand. In these monoanionic ligands, the central nitrogen atom may adopt sp^3 hybridization allowing both the phosphorus (**HL2**) or the pyridine nitrogen (**HL3**) and the iminic nitrogen atom to bond with the metal in a *fac* κ^3-coordination mode. The resulting compounds are stable saturated 18 electron species containing a strained M–N–C–N four-membered metalacycle whose inherent tension favours the thermal access to active FLP species through the breaking of one of its metal–nitrogen bonds.

In particular, we have shown that rhodium[5a,d] and iridium[5d] complexes adopting the half-sandwich geometry depicted in Scheme 1 behave as masked TMFLPs activating dihydrogen and H_2O (or D_2O) in a reversible manner, causing the gradual deuteration of the Cp* groups when D_2O was activated. However, the study of the reactivity of these phosphano– and pyridinyl–guanidino complexes has sometimes been hindered by the metalation of one of the *ortho* carbons of the *p*-tolyl group, masking the processes under study and even preventing them, in some cases.

To overcome these drawbacks, we envisaged the possibility of employing the thiourea derived **H_2L1** ligand shown in Scheme 2 in which one of the N(*p*-tolyl) groups of the guanidine moiety in **H_2L2** and **H_2L3** has been replaced by a sulphur atom. Formally, **H_2L1** retains all the desirable characteristics to generate TMFLPs and avoids the problem of orthometalation.

Herein, we report on (i) the preparation and characterization of the new complexes [(Cym)M(κ^3S,P,N-**HL1**)][SbF_6] (M = Ru (**5**), Os (**6**)), (ii) the reaction of complexes **5** and **6**, as well as that of the related ruthenium[5c] and osmium[5b] guanidinato compounds [(Cym)M(κ^3P,N,N′-**HL2**)][SbF_6] (M = Ru (**7**), Os (**8**)) and [(Cym)M(κ^3N,N′,N″-**HL3**)][SbF_6] (M = Ru (**9**), Os (**10**)) with hydrogen, (iii) the activation of water by the phosphano–guanidinato ruthenium complex **7**, (iv) DFT calculations for the activation mechanisms of dihydrogen and water and (v) the catalytic activity of complexes **5–10** in the hydrogenation of C=C, C=O or C=N bonds.

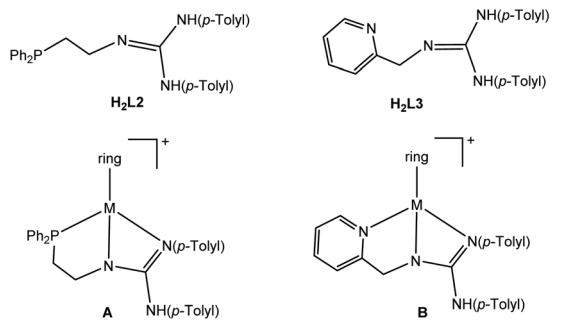

(ring)M = (η^5-C_5Me_5)Rh(III), (η^5-C_5Me_5)Ir(III), (η^6-*p*-MeC_6H_4*i*Pr)Ru(II), (η^6-*p*-MeC_6H_4*i*Pr)Os(II)

Scheme 1 Phosphano–guanidine **H_2L2** and pyridinyl–guanidine **H_2L3** ligands and derived Rh, Ir, Ru and Os complexes **A** and **B**.

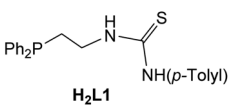

Scheme 2 The phosphano–thiourea ligand **H_2L1**.

Results and discussion

Synthesis of the complexes [(Cym)M(κ^3S,P,N-HL1)][SbF_6] (M = Ru (5), Os (6))

Reaction of the dimers [{(Cym)MCl}$_2$(μ-Cl)$_2$] (M = Ru and Os; Cym = η^6-*p*-MeC_6H_4iPr)[6] with *N*-(*p*-tolyl)-*N*′-(2-diphenylphosphanoethyl)thiourea (**H_2L1**)[7] in the presence of $NaSbF_6$ affords [(Cym)MCl(κ^2S,P-**H_2L1**)][SbF_6] (M = Ru (**1**) and Os (**2**)). Compounds **1** and **2** react with $AgSbF_6$ rendering the dicationic complexes [(Cym)M(κ^3S,P,N-**H_2L1**)][SbF_6]$_2$ (M = Ru (**3**) and Os (**4**); Scheme 3). For details about the synthesis and characterization of the ligand **H_2L1** and complexes **1–4**, see the ESI.†

Addition of solid $NaHCO_3$ to methanol solutions of complexes **3** and **4** results in partial deprotonation of the coordinated ligand **H_2L1** and formation of the monocationic complexes [(Cym)M(κ^3S,P,N-**HL1**)][SbF_6] (M = Ru, **5**; Os, **6**; Scheme 3).

A broad and weak band around 3340 cm^{-1} in the IR spectrum and a singlet at *ca*. 7.35 ppm in the ^{1}H NMR spectrum indicate the presence of the remaining NH group. An IR band

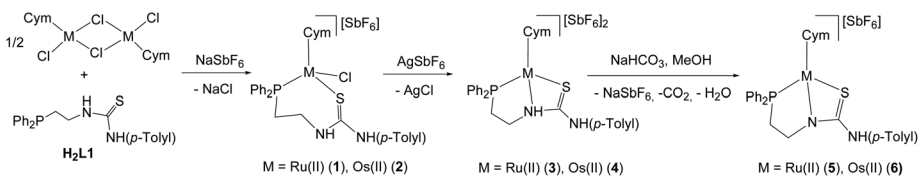

Scheme 3 Synthetic route to complexes **5** and **6**.

at around 655 cm^{-1} is attributed to the uncoordinated SbF_6 counter-anion. At room temperature, the $^{31}P\{^1H\}$ NMR spectrum consists of a singlet at 55.90 (complex **5**) and that at 21.16 ppm (complex **6**) is assigned to the phosphano substituent of the **HL1** ligand.[8]

The crystal structure of complexes **5** and **6** has been determined by single-crystal X-ray diffraction analysis. As both compounds show similar structural parameters, we will focus our discussion on the structure of the ruthenium complex **5** (for relevant structural parameters of compound **6** see the ESI†). A hexahapto coordinated Cym ring and monodeprotonated $\mathbf{H_2L1}$ acting as a *fac* κ^3S,P,N ligand make up the coordination sphere of the ruthenium cation. The metal is a stereogenic centre and the compound crystallises as a racemate. The S_{Ru} enantiomer[9] is shown in Fig. 1. As expected, bond angles within the four-membered metalacycle Ru–S(1)–C(25)–N(1) reveal the strain of this ring and, remarkably, the pyramidal arrangement around the N(1) atom ($\Sigma°N(1) = 347.1(16)°$) allows the *fac* coordination of the **HL1** ligand.

Reaction of complexes 5, 6 and [(Cym)M(κ^3-HL)][SbF_6] (HL = HL2; M = Ru (7), Os (8). HL = HL3; M = Ru (9), Os (10)) with molecular hydrogen

A common structural feature of complexes **5** and **6**, as well as of those previously reported[5b,c] **7–10** (Scheme 4), is the presence of a strained four-membered metalacycle in the cation. We assume that the cleavage of one metal–nitrogen bond within the four-membered metalacycle, favoured by the associated strain-release, could generate a TMFLP in which the metal and the nitrogen would play the role of the acidic and basic centre, respectively. Hence, complexes **5–10** could be considered as masked TMFLP species. On these grounds, we tested the reaction of these compounds with molecular hydrogen to see if they were capable of promoting the heterolytic cleavage of the hydrogen molecule showing an FLP behaviour.

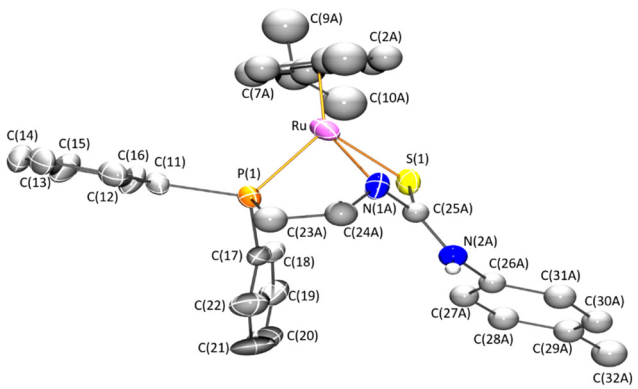

Fig. 1 Molecular structure of the cation of complex **5**. For clarity minor part of disordered fragment and all the hydrogen atoms (except that of the NH group) are omitted. Selected bond lengths (Å) and angles (°): Ru–P(1) 2.3103(13), Ru–N(1A) 2.194(14), Ru–S(1) 2.3905(15), Ru–Ct 1.6669(5), N(1A)–C(25A) 1.318(14), N(2A)–C(25A) 1.358(11); Ru–S(1)–C(25A) 84.6(3), S(1)–C(25)–N(1A) 107.0(9), S(1)–C(25A)–N(2A) 128.4(7), N(1A)–C(25A)–N(2A) 124.6(9), Ru–N(1A)–C(24A) 123.1(9), Ru–N(1A)–C(25A), 103.4(9), and C(24A)–N(1A)–C(25A) 120.6(10). Ct represents the centroid of the Cym ring.

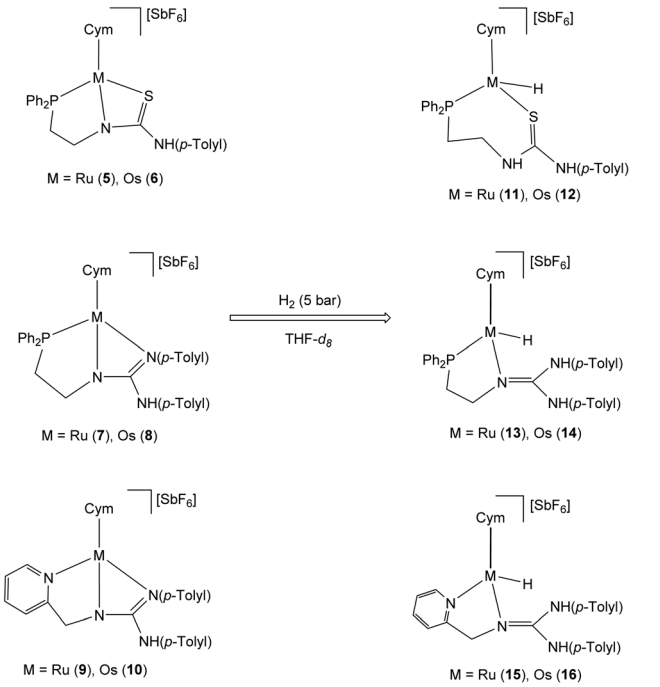

Scheme 4 Reaction with the hydrogen of complexes **5–10**.

Indeed, treatment of THF-d_8 solutions of complexes **5–10** with hydrogen gas (initial pressure, 5 bar) resulted in the formation of the corresponding metal hydrido-complexes [(Cym)MH(κ^2-$\mathbf{H_2L}$)][SbF_6] (**11–16**; Scheme 4). Formally, the heterolytic cleavage of the molecule of hydrogen gives rise to hydridic M–H and protic N–H bonds. It is notable that while in the phosphano–guanidino compounds **7** and **8** and in the pyridinyl–guanidino complexes **9** and **10** the metal–imino nitrogen bond is broken, with subsequent protonation of the resulting N(*p*-tolyl) group, in the reaction with hydrogen of the phosphano–thiourea compounds **5** and **6**, the cleavage of the metal–imidic nitrogen bond takes place and the metal–sulfur bond remains intact (Scheme 4).[10]

Slow reaction rates were observed. Several hours to some days of reaction are necessary to achieve complete conversion working in the 298–373 K range of temperature (see the Experimental section). In the hydrogenation of the pyridinyl–guanidino compounds **9** and **10**, the concomitant formation of an orthometalated compound in 10% and 20% molar ratio, respectively, was observed. For the alternative preparation and characterisation of these orthometalated side-products (compounds **17** and **18**) see the following.

Hydrogenation is reversible. Fig. 2 shows the evolution of the $^{31}P\{^1H\}$ spectrum of a sample of complex **5** after treatment with molecular hydrogen and, then, after the hydrogen pressure was removed. In the absence of hydrogen, the hydrogenation product **11** spontaneously converts completely into starting compound **5**, after 6 days at 363 K. Due to the reversibility of the reaction, removing of volatiles from the reaction

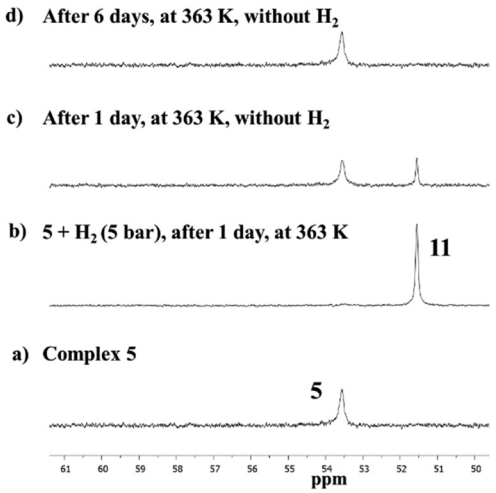

Fig. 2 Reversible hydrogenation of complex **5**. The $^{31}P\{^1H\}$ spectrum of (a) starting complex **5**; (b) after 1 day of treatment with H_2 (5 bar) at 363 K, (c) after one more day in the absence of H_2, (d) after 5 more days without H_2.

medium mostly afforded the starting materials sometimes containing variable amounts of the corresponding hydrido compounds. For this reason, to obtain satisfactory NMR data for the hydrido compounds, spectra have to be recorded under hydrogen pressure.

Two singlets in the 6.64–9.53 ppm region of the ^1H NMR spectrum of complexes **11–16** are indicative of the presence of two NH functionalities in the molecule. A signal in the high field region of the ^1H NMR spectrum is attributed to the hydrido ligand. For the phosphano–thiourea and phosphano–guanidino compounds **11–14** this signal appears as a doublet, due to the coupling to the phosphorus nucleus in the −8.83 to −10.30 ppm region. For the pyridinyl–guanidino complexes **15** and **16** a singlet at −5.34 and −5.29 ppm, respectively, is assigned to the metal–hydrido resonance. At room temperature, the $^{31}P\{^1H\}$ spectrum of complexes **11–14** consists of one singlet confirming the presence of the PPh_2 group in the cation.

The crystal structure of complexes **13** and **14** was elucidated by X-ray diffraction analysis. Both compounds have been found to be isostructural, crystallising in the centrosymmetric $P2_1/c$ space group with two independent molecules in their asymmetric unit. One of the independent cations of compound **13** is depicted in Fig. 3. It shows a three-legged piano stool geometry formed by the η^6-coordinated Cym fragment, the hydrido and the **H_2L2** ligand κ^2 P,N coordinated (an analogous representation of complex **14** is included in the ESI†). Geometrical parameters of the CN_3 guanidine fragment indicate a slight partial double character for the two C–NH(*p*-tolyl) bonds [N(2)–C(25) 1.364(3), N(3)–C(25) 1.367(3)] together with a comparatively shorter distance of the C(25)–N(1) bond [N(1)–C(25) 1.304(3)]. A planar geometry around the coordinated nitrogen of the phosphano–guanidine ligand [Σ°N(1) = 360 (3)°] was determined.

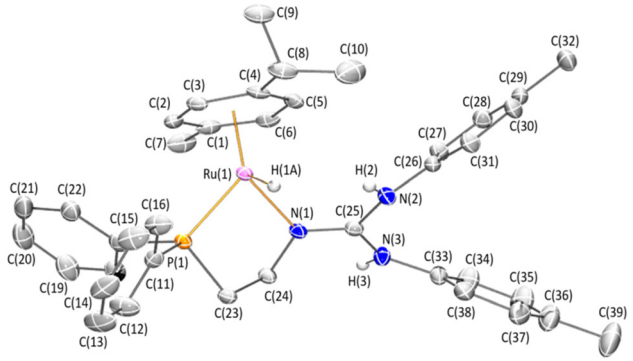

Fig. 3 Molecular structure of one of the two crystallographically independent cations of complex **13**. For clarity all the hydrogen atoms, except for the hydrido and hydrogen atoms of NH groups, together with minor component of disordered fragments are omitted. Selected bond lengths (Å) and angles (°): Ru(1)–N(1) 2.1245(17), Ru(1)–P(1) 2.2645(6), Ru(1)–H(1A) 1.608, Ru(1)–Ct(1) 1.7397(1), N(1)–C(25) 1.304(3), N(2)–C(25) 1.364(3), N(3)–C(25) 1.367(3), Ct(1)–Ru(1)–N(1) 130.36(1), Ct(1)–Ru(1)–P(1) 133.54(1), Ct(1)–Ru(1)–H(1) 120, P(1)–Ru(1)–N(1) 81.63(5), P(1)–Ru(1)–H(1A) 88.2, and N(1)–Ru(1)–H(1A) 88.4. Ct represents the centroid of the Cym ring.

DFT calculations for the hydrogenation of complex 7

The Gibbs free energy profiles for the hydrogenation of **7** were calculated by DFT methods, at the B3LYP-D3/311G(d,p)/LanL2TZ(f) level (see the ESI†). Fig. 4 shows the intermediates and transition states along with the relative Gibbs free energies for the process. Dissociation of the terminal Ru–N bond of **7** affords the true TMFLP species **A** through the transition state **TS_7-A**. Intermediate **A** interacts with H_2 rendering **A**·H_2 in which the hydrogen molecule approximates one of its hydrogen atoms to the free nitrogen (N···H: 2.593 Å). Subsequently,

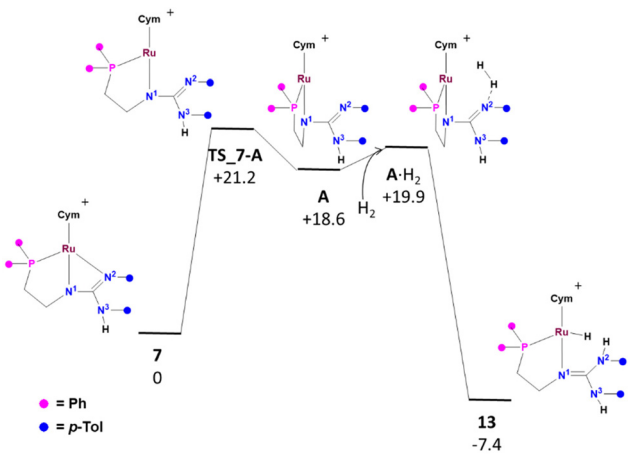

	7	A	A·H_2	13
C–N1	1.359	1.418	1.417	1.313
C–N2	1.327	1.287	1.288	1.366
C–N3	1.365	1.383	1.381	1.368

Fig. 4 Gibbs free energy profile (kcal mol^{-1}) for the reaction with hydrogen of complex **7** [B3LYP-D3/311G(d,p)/LanL2TZ(f) level, in THF (SMD), 298 K].

the formation of an N–H bond and coordination of the remaining hydrogen atom with the metal with the concomitant H–H bond rupture yield hydride complex **13**. The activation Gibbs free energies of the direct and reverse processes (21.2 and 28.6 kcal mol^{-1}, respectively) are coherent with the slow experimental reaction rates observed and parallel to those proposed for main group FLPs[11a,b] and TMFLPs.[11c] The electronic rearrangement that takes place throughout the hydrogenation process is remarkable. Indeed, the CN bond distances suggest that while the C–N3 bond remains single throughout the process (Fig. 4), the C–N1 and C–N2 bonds change from single to double and from double to single, respectively going from **7** to **13**.

Orthometalation reactions

Heating methanol solutions of [(Cym)M(κ^{3}N,N′,N″-**HL3**)][SbF_6] (M = Ru (**9**), Os (**10**)) at 338 K affords the orthometalated complexes [(Cym)M(κ^{3}N,N′,C-$\mathbf{H_2L3_{-H}}$)][SbF_6] (M = Ru (**17**), Os (**18**)), respectively (Scheme 5).

As the most relevant NMR data, the ^{1}H NMR spectrum in CD_2Cl_2, shows two singlets at 7.09 and 6.54 ppm for complex **17** and at 7.09 and 6.49 ppm for **18** that denote the presence of two inequivalent NH groups. In addition, a singlet at 151.47 (**17**) and at 140.26 (**18**) ppm in the ^{13}C{^{1}H} NMR spectrum is assigned to the corresponding M–C carbon resonance.

Single crystals of **17** were grown from methanol/diethyl ether/*n*-pentane solutions. The complex crystallises with two crystallographically independent, but chemically identical molecules in the unit cell. As only slight structural differences are found between them, description will be focused on one of them. The cation exhibits a three-legged-piano stool geometry with an η^6 coordinated Cym ligand. The metalated pyridinyl–guanidine ligand occupies three mutually *cis* positions at the metal centre rendering two fused metalacycles, namely the five-membered ring Ru(1)–N(1)–C(15)–C(16)–N(2) and the six-membered ring Ru(1)–N(2)–C(17)–N(3)–C(18)–C(19). The metal centre is stereogenic and, as the molecule crystallises in the centrosymmetric space group $P\bar{1}$, both enantiomers, namely S_{Ru} (shown in Fig. 5) and R_{Ru}, are present in the unit cell. In the formation of complexes **17** and **18** from **9** and **10**, new metal–carbon and N–H bonds form and, hence, formally speaking, the metalation reaction involves the activation of an aromatic C(sp^2)–H bond by metal–ligand cooperation. Seemingly, these structural features are closely related to the formation of a less strained six-membered ring in **17** instead of the four-membered ring present in the starting materials.

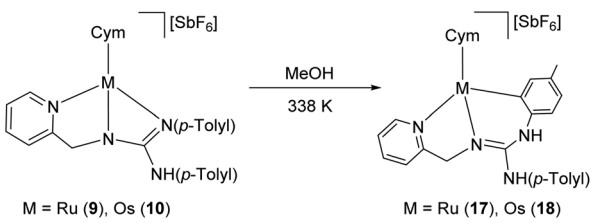

M = Ru (**9**), Os (**10**) M = Ru (**17**), Os (**18**)

Scheme 5 Preparation of the orthometalated complexes **17** and **18**.

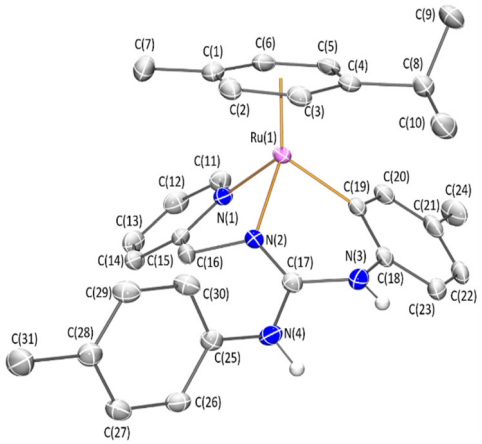

Fig. 5 Molecular structure of one of the two crystallographically independent cations of complex **17**. For clarity all the hydrogen atoms are omitted, except those of NH groups. Selected bond lengths (Å) and angles (°): Ru–N(1) 2.0914(19), Ru–N(2) 2.0781(19), Ru–C(19) 2.069(2), Ru–Ct 1.7118(1), N(2)–C(17) 1.305(3), N(3)–C(17) 1.358(3), N(4)–C(17) 1.372(3), Ct–Ru–N(1) 127.57(1), Ct–Ru–N(2) 132.45(1), Ct–Ru–C(19) 129.28(1), N(1)–Ru–N(2) 76.18(7), N(1)–Ru–C(19) 90.05(8), and N(2)–Ru–C(19) 83.67(8). Ct represents the centroid of the Cym ring.

Water and C(sp^3)–H bond activation by the phosphano–guanidino complex 7

The phosphano–guanidino compound [(Cym)Ru(κ^{3}P,N,N′-**HL2**)][SbF_6] (**7**) activates the polar O–H bond of water. Although addition of excess of water to THF solutions of complex **7** does not produce significant changes in its ^{1}H and ^{31}P NMR spectra, NMR and mass spectrometry measurements clearly indicate that complex **7** reacts with deuterated water in a reversible fashion resulting in the complete deuteration of the Me group of the Cym ligand. The ^{31}P{^{1}H} NMR spectrum of THF-d_8/D_2O (75%/25%, v/v) solutions does not change over time but the ^{1}H NMR spectrum shows a gradual decrease of the singlet attributed to the Me protons of the Cym ligand together with the concurrent appearance of a broad signal at almost the same chemical shift (Fig. 6a). The concomitant variation of the mass spectra of the cation of **7** over time is shown in Fig. 6b. This whole set of data evidences the progressive deuteration of the methyl protons of the Cym ring. The deuteration process is clean, with only isotopologues of compound **7** with different degrees of deuteration being detected by NMR spectroscopy.

A few examples of related H/D exchanges involving the methyl groups of the Cp* ligand in half-sandwich rhodium(III) or iridium(III) complexes have been reported.[5a,d,12] Usually, the intervention with a strong external base is necessary[12a–d] but mediation of the basic component of an FLP species can also promote this exchange.[5a,d,12e] However, under similar conditions, deuteration of the methyl protons of the Cp* ligand was not observed in Cp*Ru(II) homologues[12b] and, as far as we know, no cases of methyl proton deuteration of Cym ligands have been described so far. Notably, the H/D exchange observed in **7** does not need the addition of an external base.

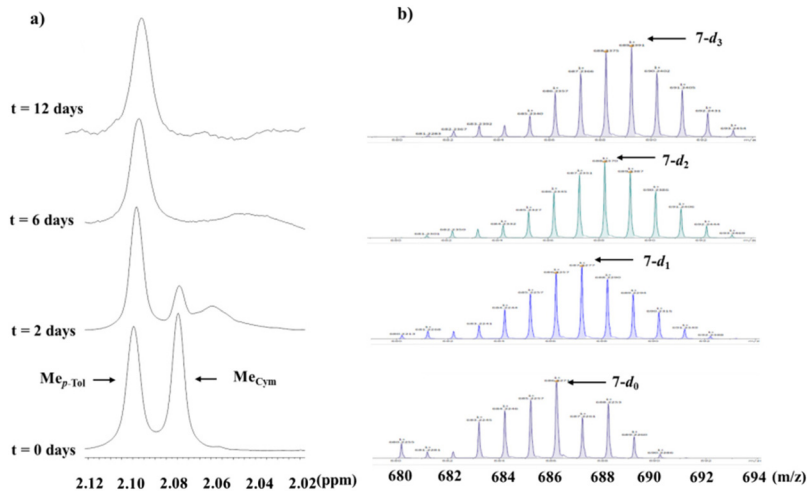

Fig. 6 Evolution of the ^{1}H NMR spectra (a) and of the mass spectra (b) of solutions of complex **7** in THF-d_8/D_2O (75%/25%, v/v).

Kinetic measurements indicate that the deuteration process obeys a pseudo-first-order rate law with k_{obs} values from 3.88 × 10^{-5} to 2.32 × 10^{-4} s^{-1}, in the 358–373 K temperature range. The linear fitting of $\ln(k_{obs}/T)$ *versus* $1/T$ gives a $\Delta G^{\ddagger}$ value of 28(1) kcal mol^{-1} at 273 K. The formation of 7-d_3 from **7** is reversible. At 358 K, a THF-d_8/H_2O (75%/25%, v/v) solution of 7-d_3 evolves to **7** with an observed pseudo-first-order rate constant of 0.65 × 10^{-5} s^{-1} (see the ESI†). The high measured ratio, $k_H/k_D \approx 6$, indicates that the rate-determining step for the exchange process is the C–H(D) bond cleavage.

The mechanism of this H/D exchange process was explored by DFT calculations in order to shed light on the deuteration of **7** in the presence of D_2O. Fig. 7 shows the Gibbs free energy profile together with the involved intermediates and transition states. Formation of the unsaturated TMFLP species **A** has been discussed above. **A** reacts with H_2O giving the species **A**·H_2O in which the incoming water molecule forms an N2···H1–O hydrogen bond [N2···H1: 1.888 Å, O–H1: 0.985 Å, N2···O: 2.872 Å, N2–H1–O: 176.7°]. The Ru–O distance, 3.470 Å, excludes any significant metal–hydroxo bond interaction. Intermediate **A**·H_2O evolves to **B** that contains an O–H ligand (Ru–O: 2.091 Å) and a N2–H1···O hydrogen bond [N2–H1: 1.040 Å, O···H1: 1.726 Å, N2···O: 2.697 Å, N2–H1–O: 153.6°]. The transition state from **A**·H_2O to **B**, **TS_A-B**, shows a geometry rather similar to **A**·H_2O, with the N2···H1 distance shortened to 1.795 Å. Finally, **B** evolves to the methylene cyclohexenyl ruthenium(II) derivative through the transition state **TS_B–C**. The newly formed water molecule in **C** is bound to

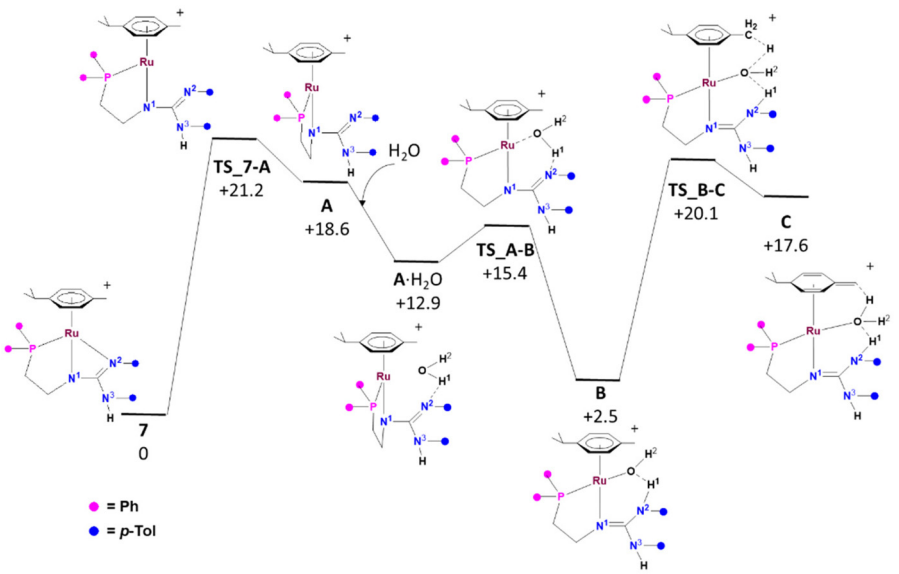

Fig. 7 Gibbs free energy profile [B3LYP-D3/311G(d,p)/LanL2TZ(f) level, in THF (SMD), 298 K] for the hydrogen exchange at the methyl Cym ligand of complex **7**.

the ruthenium with a rather long Ru–O bond (2.326 Å); a search in the Cambridge Structural Database (CSD)[13] for (Cym)RuOH$_2$ fragments showed Ru–OH$_2$ bond distances between 2.118 and 2.204 Å, with a mean value of 2.146 Å. An N2–H1···O hydrogen bond is still present [N2–H1: 1.016 Å, O···H1: 1.949 Å, N2···O: 2.925 Å, N2–H1–O: 160.4°]. The calculated Gibbs free energy profile (Fig. 7) indicates that the formation of species **C** should be reversible. Therefore, the H/D exchange process under discussion should result in the progressive H/D exchange at the methyl of the Cym ligand.

In summary, complex **7** belongs to the class of thermally induced FLPs (masked FLP) and presents the advantage of being air and moisture stable. The existence of a strong ring strain within the Ru–N–C–N four-membered cycle most probably facilitates the reversible cleavage of the Ru–N(sp^2) bond and makes accessible frustrated Lewis pair sites available for the reversible activation of both polar, H–O–H, and nonpolar, H_2, bonds. When D_2O was employed, the generated Ru–OD intermediate is responsible for an unprecedented H/D exchange of the methyl protons of the Cym ligand.

Catalytic hydrogenation assays

The masked FLP complexes **5–10** have been tested as catalysts in the hydrogenation of the C=C double bond of styrene and a range of acrylates, the C=O bond of acetophenone and the C=N bond of *N*-benzylideneaniline and quinoline. Under the standard conditions employed (5 bar hydrogen, 5 mol% catalyst loading, at 363 K in THF as the solvent) all the complexes are active catalysts in all the tested hydrogenations. However, slow hydrogenation rates were observed, several hours (even a few days) being needed to achieve complete conversion (see the ESI†). Both, the starting complex **5–10** and the corresponding hydrido compounds **11–16** were detected under catalytic conditions indicating that both the hydrogenation of the catalyst and the hydrogen transfer to the substrate are slow steps in the catalytic cycle. Side reactions also affect negatively the catalytic outcome. Thus, when complexes **9** and **10** were used as catalysts, variable amounts of the corresponding metalated complexes **17** and **18** (see the Experimental section and the ESI†) were detected. Additionally, when the hydrogenation of methyl acrylate was mediated by the pyridinyl–guanidino ruthenium compound **9**, single-crystals of the complex **19** were isolated from the catalytic medium.

Fig. 8 shows a view of the cation of complex **19** including a selection of the bond lengths and angles of the complex. Along with the η^6-Cym arene ligand, a *fac* κ^3N,N′,C coordinated ligand completes the coordination sphere of the metal. Scheme 6 shows a plausible explanation for the formation of this trihapto ligand. Cleavage of the Ru–N(*p*-tolyl) bond of the masked FLP **9** affords active FLP **9A** in equilibrium with its tautomer **9B** whose formation involves the dearomatisation of the pyridine ring of the ligand. Reaction with methyl acrylate, accompanied by the rearomatisation of the pyridine ring, gives complex **19**. The proposed path for the formation of complex **19** from **9** indicates that the C=C double bond of olefins bearing electron-withdrawing groups can be activated by

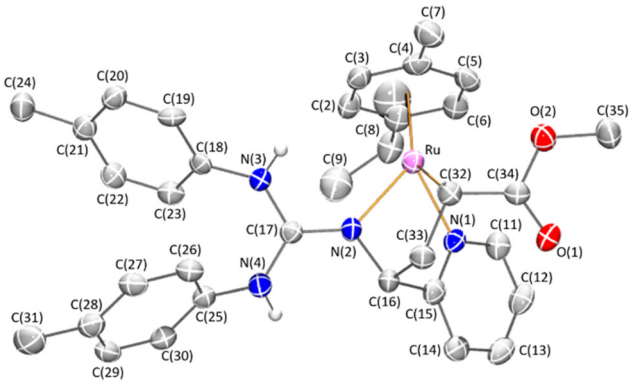

Fig. 8 Molecular structure of the cation of the complex **19**. For clarity all the hydrogen atoms are omitted, except for those of NH bonds. Selected bond lengths (Å) and angles (°): Ru–N(1) 2.110(5), Ru–N(2) 2.088(5), Ru–C(32) 2.203(7), Ru–Ct 1.704(3), N(2)–C(17) 1.320(8), N(3)–C(17) 1.355(8), N(4)–C(17) 1.358(8), Ct–Ru–N(1) 131.83(16), Ct–Ru–N(2) 135.43(17), Ct–Ru–C(32) 131.5(2), N(1)–Ru–N(2) 76.6(2), N(1)–Ru–C(32) 82.1(2), and N(2)–Ru–C(32) 77.5(5). Ct represents the centroid of the Cym ring.

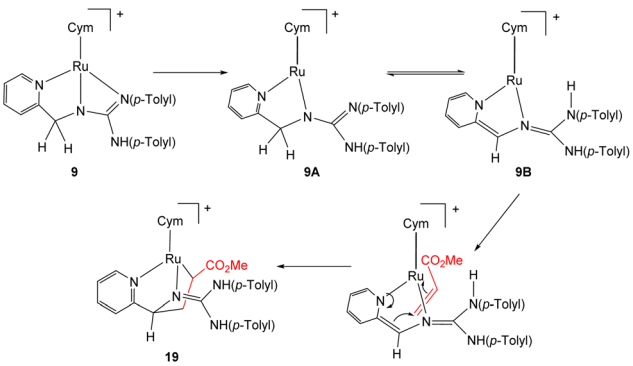

Scheme 6 Proposed formation pathway of complex **19** from **9**.

complex **9** following a metal–ligand cooperative dearomatisation/aromatisation mechanism.[14]

In complex **19**, the ruthenium atom and the carbon atoms C(16) and C(32) (see Fig. 8) are stereogenic centres. The configuration of the C(16) carbon is predetermined by the configuration at the metal: the *R* configuration at the ruthenium exclusively induces *R* configuration at the C(16) carbon and *vice versa*. However, in principle, the C(32) carbon may freely adopt both *R* and *S* configurations. Hence, diastereomers of configuration R_{Ru},$R_{C(16)}$,$R_{C(32)}$ and R_{Ru},$R_{C(16)}$,$S_{C(32)}$ and their corresponding enantiomers S_{Ru},$S_{C(16)}$,$S_{C(32)}$ and S_{Ru},$S_{C(16)}$,$R_{C(32)}$ can be obtained. Indeed, the ^{1}H NMR spectrum of the detected compound **19** shows the presence of two diastereomers in about 55/45 molar ratio. The complex crystallises in the chiral $P2_12_12_1$ space group of the orthorhombic crystal system and only the R_{Ru},$R_{C(16)}$,$S_{C(32)}$ isomer,[9] depicted in Fig. 8, is present in the unit cell. Therefore, the compound crystallises as a conglomerate.[15] The other diastereomer

detected in solution by ^{1}H NMR spectroscopy has to be (R_{Ru},$R_{C(16)}$,$R_{C(32)}$)-**19**.

Notably, the CO_2Me protons of the minor diastereomer are strongly shielded ($\delta(CO_2Me)_m$, 3.21 ppm) with respect to those of the major diastereomer ($\delta(CO_2Me)_M$, 3.88 ppm). We assume that this shielding is produced by the diamagnetic current of the pyridinyl ring of the trihapto ligand and, therefore, the configuration of the C(32) carbon in the minor diastereomer has to be *S*, because only in this configuration the CO_2Me group can be affected by the pyridinyl ring current. Consequently, the configuration of the most abundant isomer in solution is (R_{Ru},$R_{C(16)}$,$R_{C(32)}$)-**19**.

Conclusions

Phosphano–thiourea **H_2L1**, phosphano–guanidino **H_2L2** and pyridinyl–guanidino **H_2L3** derivatives are well suited for the preparation of masked FLPs containing ruthenium and osmium fragments as the acidic component and nitrogen as the basic counterpart. The derived species **5–10** activate molecular dihydrogen following FLP pathways. The phosphano–guanidino complex **7** activates deuterated water and the resulting nucleophilic Ru–OD containing fragment is able to abstract a proton of the methyl group of the *p*-cymene ligand. The reversibility of the process results in the sequential H/D exchange up to complete deuteration of this methyl group. One of the *p*-tolyl groups of complexes **9** and **10** undergoes the metalation reaction of one of its *ortho* C(sp^2)–H bonds rendering the saturated compounds **17** and **18**. The C=C double bond of methyl acrylate diastereoselectively adds to the ruthenium complex **9**, giving rise to new C–C and Ru–C bonds. Remarkably, the study of the reactivity of TMFPL species with H_2 and H_2O has allowed us to detect the activation of a variety of chemical bonds (H–H, O–H, C(sp^3)–H, C(sp^2)–H and C(sp^2)=C(sp^2)) by metal–ligand cooperation mechanisms. DFT calculations support the FLP behaviour of the complexes in both hydrogen and water activation.

Experimental

All preparations have been carried out under argon. All solvents were treated in a PS-400-6 Innovative Technologies Solvent Purification System (SPS) and degassed prior to use. Infrared spectra were recorded on a PerkinElmer Spectrum-100 (ATR mode) FT-IR spectrometer. Carbon, hydrogen and nitrogen analyses were performed using a PerkinElmer 240 B microanalyser. ^{1}H, ^{13}C and ^{31}P NMR spectra were recorded on a Bruker AV-300 spectrometer (300.13 MHz), Bruker AV-400 (400.16 MHz) or Bruker AV-500 (500.13 MHz). In both ^{1}H NMR and ^{13}C NMR measurements the chemical shifts are expressed in ppm downfield from $SiMe_4$. The ^{31}P NMR chemical shifts are relative to 85% H_3PO_4. *J* values are given in Hz. COSY, NOESY, HSQC and HMBC ^{1}H–X (X = ^{1}H, ^{13}C, ^{31}P) correlation spectra were obtained using standard procedures. Mass spectra were obtained with a Micro Tof-Q Bruker Daltonics spectrometer.

Preparation of the complexes [(Cym)M(κ^{3}S,P,N-HL1)][SbF$_6$] (M = Ru (5), Os (6))

To a solution of the corresponding complex [(Cym)M(κ^{3}S,P,N-**H_2L1**)][SbF$_6$]$_2$ (0.50 mmol) in methanol (20 mL), 42.6 mg (0.50 mmol) of solid $NaHCO_3$ were added. The resulting suspension was stirred for 24 h and then vacuum-evaporated to dryness. The residue was extracted with dichloromethane and the resulting solution was concentrated under reduced pressure to *ca.* 2 mL. The slow addition of *n*-pentane led to the precipitation of an orange (complex **5**) or yellow (complex **6**) solid, which was washed with *n*-pentane (3 × 5 mL) and vacuum-dried. Crystals of **5** and **6** suitable for X-ray diffraction analysis were obtained by crystallisation from CH_2Cl_2/*n*-pentane (**5**) or CH_2Cl_2/*n*-hexane (**6**) solutions.

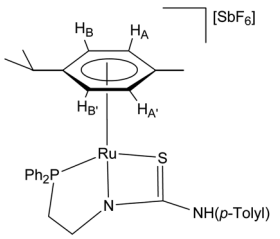

5

Complex 5. Yield: 330.9 mg, 78%. Anal. calcd for $C_{32}H_{36}N_2F_6PRuSSb$: C, 45.3; H, 4.3; N, 3.3; S, 3.8. Found: C, 45.0; H, 4.5; N, 3.0; S, 3.9. HRMS (μ-TOF), $C_{32}H_{36}N_2PRuS$, [M – SbF$_6$]$^+$, calcd: 613.1375, found: 613.1361. IR (cm^{-1}): ν(NH) 3347 (w), ν(SbF$_6$) 655 (s). ^{1}H NMR (500.10 MHz, CD_2Cl_2, RT): δ = 7.65–7.35 (m, 10H, PPh_2), 7.38 (s, 1H, NH), 7.02, 6.68 (AB system, *J*(A,B) = 8.4 Hz, 4H, *p*-tolyl), 5.66, 5.47 (AB system, *J*(A,B) = 6.2 Hz, 2H, H_A, H_B, Cym), 5.25 5.06 (AB system, *J*(A,B) = 5.9 Hz, 2H, $H_{A'}$, $H_{B'}$, Cym), 4.06 (dm, *J* = 40.0 Hz, 1H, NCH_2), 3.28 (m, 1H, NCH_2), 2.73 (m, 2H, PCH_2), 2.64 (sp, 1H, CH iPr), 2.27 (s, 3H, Me *p*-tolyl), 2.13 (s, 3H, Me Cym), 1.29 (d, *J* = 6.9 Hz, 3H, Me iPr), 1.26 (d, *J* = 6.9 Hz, 3H, Me iPr). ^{13}C{^{1}H} NMR (125.77 MHz, CD_2Cl_2, RT): δ = 185.51 (C=S), 138.07 (d, *J* = 47.2 Hz), 135.14–129.51 (PPh_2), 137.08 (*C*Me), 133.69 (CN), 130.43 (CH_3, CH_5), 129.91 (d, *J* = 46.3 Hz), 123.81 (CH_2, CH_6) (*p*-tolyl), 111.52 (*C*–iPr, Cym), 102.24 (*C*–Me, Cym), 91.74 (d, *J* = 6.4 CH_A), 90.48 (d, *J* = 4.1 CH_B), 89.70 (d, *J* = 3.1 $CH_{B'}$), 88.05 ($CH_{A'}$), 53.50 (d, *J* = 4.8, CH_2N), 32.01 (d, *J* = 35.1, CH_2P), 31.12 (CH iPr), 22.55, 22.15 (Me iPr), 19.98 (Me *p*-tolyl), 18.18 (Me Cym). ^{31}P{^{1}H} NMR (202.46 MHz, CD_2Cl_2, RT): δ = 55.90 (s).

^{31}P{^{1}H} NMR (202.46 MHz, CD_2Cl_2, 173 K): δ = 66.61(bs), 61.12 (bs), 56.64 (bs).

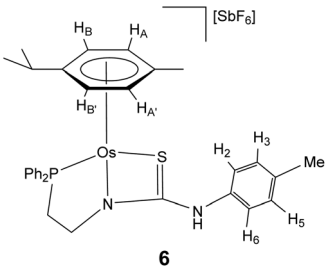

6

Complex 6. Yield: 365.7 mg, 78%. Anal. calcd for $C_{32}H_{36}N_2F_6OsPSSb$: C, 41.0; H, 3.9; N, 3.0; S, 3.4. Found: C, 40.9; H, 3.9; N, 2.9; S, 3.6. HRMS (μ-TOF), $C_{32}H_{36}N_2OsPS$, $[M - SbF_6]^+$, calcd: 703.1946, found: 703.1943. IR (cm^{-1}): ν(NH) 3336 (w), $\nu(SbF_6)$ 654 (s). ^1H NMR (500.10 MHz, CD_2Cl_2, RT): δ = 7.64–7.28 (m, 10H, PPh_2), 7.34 (s, 1H, NH), 7.00 (A part of an AB system, 2 H, H_3, H_5), 6.73 (B part of an AB system, J(A,B) = 8.2 Hz, 2 H, H_2, H_6, *p*-tolyl), 5.75 (d, J = 5.9 Hz, 1H, H_B), 5.49 (d, 1H, H_A), 5.25 (bs, 1H, $H_{B'}$), 5.17 (d, J = 5.8 Hz, 1H, $H_{A'}$), 4.08 (dm, J = 27.4 Hz, 1H), 3.17 (m, 1H (NCH_2)), 2.75, 2.60 (2 × m, 2H, PCH_2), 2.60 (m, 1H, CH iPr), 2.25 (s, 3H, Me *p*-tolyl), 2.23 (s, 3H, Me Cym), 1.29 (d, J = 7.0 Hz, 3H, Me iPr), 1.24 (d, J = 6.9 Hz, 3H, Me iPr). $^{13}C\{^1H\}$ NMR (125.77 MHz, CD_2Cl_2, RT): δ = 191.75 (C═S), 137.58 (d, J = 55.9 Hz), 135.46–129.56, 128.77 (d, J = 53.0 Hz) (PPh_2), 137.04, 133.23, 130.39 (CH_3, CH_5), 123.43 (CH_2, CH_6) (*p*-tolyl), 102.72 (*C*–Me, Cym), 93.78 (*C*–iPr, Cym), 83.84 (d, J = 6.5 Hz, CH_A), 83.09 (d, J = 4.2 Hz, CH_B), 82.04 ($CH_{B'}$), 79.51 ($CH_{A'}$), 56.63 (d, J = 3.6 Hz, CH_2N), 34.35 (d, J = 40.5 Hz, CH_2P), 32.82 (CH iPr), 24.15, 23.75 (Me iPr), 21.39 (Me *p*-tolyl), 19.30 (Me Cym). $^{31}P\{^1H\}$ NMR (202.46 MHz, CD_2Cl_2, RT): δ = 21.16 (s).

$^{31}P\{^1H\}$ NMR (202.46 MHz, CD_2Cl_2, 173 K): δ = 32.83 (bs), 26.84 (bs), 22.81 (bs).

Formation of the complexes [(Cym)MH(κ²-H₂L)][SbF₆] (H₂L = H₂L1, M = Ru (11), Os (12); H₂L = H₂L2, M = Ru (13), Os (14); H₂L = H₂L3, M = Ru (15), Os (16))

A high-pressure NMR tube containing a solution of the corresponding [(Cym)M(κ³-**HL**)][SbF_6] (**5–10**; 0.045 mmol) in THF-d_8 (0.45 mL), was pressurised with H_2 (5 bar) and the resulting solution was monitored by NMR spectroscopy. After several hours of reaction at temperatures ranging from 298 to 373 K (24 h at 263 K (**5**), 5 days at 273 K (**6**), 17 h (**7**) and 22 h (**8**) at 263 K, and 18 h (**9**) and 22 h (**10**) at 298 K) complete conversion was achieved in all cases. The resulting hydrido complexes [(Cym)MH(κ²-**H₂L**)][SbF_6] (**11–16**) were characterised by NMR spectroscopy, under H_2 pressure. Crystals suitable for X-ray diffraction analysis were obtained by crystallisation from THF/diethyl ether/*n*-pentane (complex **13**) and dichloromethane (complex **14**) solutions.

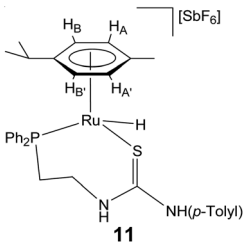

11

Complex 11. HRMS (μ-TOF), for $C_{32}H_{38}N_2PRuS$, $[M - SbF_6]^+$, calcd: 615.1531, found: 615.1522. ^1H NMR (500.10 MHz, THF-d_8, RT): δ = 9.49 (s, 1H, *p*-tolylN*H*), 7.84–7.38 (m, 10H, PPh_2), 7.18 (t, J = 6.5 Hz, 1H, CH_2NH), 7.09, 6.49 (AB system, J = 8.1 Hz, 4H, *p*-tolyl), 6.01, 5.24 (AB system, J = 6.4 Hz, 2H, H_A, H_B, Cym), 5.55, 4.39 (AB system, J = 5.6 Hz, 2H, $H_{A'}$, $H_{B'}$, Cym), 4.22, 4.07 (2 × m, 2H, NCH_2), 2.94, 2.67 (2 × m, 2H, PCH_2), 2.28 (s, 3H, Me *p*-tolyl), 2.13 (s, 3H, Me Cym), 1.91 (sp, 1H, CH iPr), 1.28 (d, J = 6.8 Hz, 3H, Me iPr), 1.10 (d, J = 6.9 Hz, 3H, Me iPr), −9.32 (d, J = 47.2 Hz, 1H, Ru–H). $^{13}C\{^1H\}$ NMR (125.77 MHz, THF-d_8, RT): δ = 179.45 (C═S), 138.12 (d, J = 50.9 Hz), 136.39 (d, J = 45.2 Hz), 133.62–128.94 (PPh_2), 138.07 (*C*Me), 133.90 (CN), 130.80 (CH_3, CH_5), 125.67 (CH_2, CH_6) (*p*-tolyl), 110.22 (*C*–iPr, Cym), 108.26 (*C*–Me, Cym), 93.71 (d, J = 5.2 CH_A), 92.53 ($CH_{A'}$), 89.42 (d, J = 6.1 CH_B), 85.45 ($CH_{B'}$), 43.69 (CH_2N), 32.14 (d, J = 31.7, CH_2P), 25.09 (CH iPr), 24.53, 22.75 (Me iPr), 20.69 (Me *p*-tolyl), 18.26 (Me Cym). $^{31}P\{^1H\}$ NMR (202.46 MHz, THF-d_8, RT): δ = 51.53 (s).

$^{31}P\{^1H\}$ NMR (202.46 MHz, THF-d_8, 173 K): δ = 55.78 (bs), 52.04 (bs).

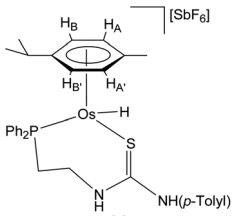

12

Complex 12. HRMS (μ-TOF), $C_{32}H_{38}N_2OsPS$, $[M - SbF_6]^+$, calcd: 705.2137, found: 705.2103. ^1H NMR (500.10 MHz, THF-d_8, RT): δ = 9.53 (s, 1H, *p*-tolylN*H*), 7.81–7.33 (m, 10H, PPh_2), 7.28 (t, 1H, CH_2NH), 7.10, 6.53 (AB system J = 7.7 Hz, 4H, *p*-tolyl), 5.80, 5.07 (AB system, J = 6.2 Hz, 2H, H_A, H_B, Cym), 5.44, 4.27 (AB system, J = 5.2 Hz, 2H, $H_{A'}$, $H_{B'}$, Cym), 4.37, 3.94 (2 × m, 2H, NCH_2), 3.20, 2.77 (2 × m, 2H, PCH_2), 2.28 (s, 3H, Me *p*-tolyl), 2.26 (s, 3H, Me Cym), 1.90 (sp, 1H, CH iPr), 1.26 (d, J = 6.9 Hz, 3H, Me iPr), 1.14 (d, J = 6.9 Hz, 3H, Me iPr), −10.30 (d, J = 39.2 Hz, 1H, Os–H). $^{13}C\{^1H\}$ NMR (125.77 MHz, THF-d_8, RT): δ = 177.49 (C═S), 138.65 (d, J = 55.78 Hz), 135.04 (d, J = 49.9 Hz), 134.05–128.81 (PPh_2), 138.10 (*C*Me), 130.83 (CH_3, CH_5), 125.60 (CH_2, CH_6) (*p*-tolyl), 101.52 (*C*–iPr, Cym), 101.15 (*C*–Me, Cym), 85.96 (d, J = 5.3 CH_A), 84.37 ($CH_{A'}$), 80.38 (d, J = 6.3 CH_B), 76.81 ($CH_{B'}$), 44.10 (CH_2N), 32.31 (d, J = 36.6, CH_2P), 31.52 (CH iPr), 24.58, 24.27 (Me iPr), 20.72 (Me *p*-tolyl), 17.67 (Me Cym). $^{31}P\{^1H\}$ NMR (202.46 MHz, CD_2Cl_2, RT): δ = 5.64 (s).

$^{31}P\{^1H\}$ NMR (202.46 MHz, THF-d_8, 193 K): δ = 9.41 (bs), 7.00 (bs).

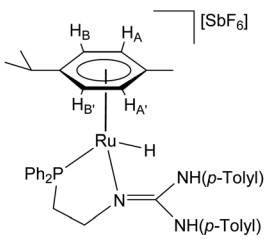

13

Complex 13. HRMS (μ-TOF), $C_{39}H_{45}N_3PRu$, $[M - SbF_6]^+$, calcd: 688.2439, found: 688.2422. ^1H NMR (500.10 MHz, THF-d_8, RT): δ = 8.31 (s, 1H, NH *trans* Ru), 7.80–7.40 (m, 10H,

PPh_2), 7.35 (s, 1H, NH *trans* CH_2), 7.12, 7.10, 6.99, 6.87 (4 × d, J = 8.4 Hz, 8H, *p*-tolyl), 5.40, 5.37 (AB system, J = 6.2 Hz, 2H, H_A, H_B, Cym), 5.24, 5.18 (AB system, J = 5.9 Hz, 2H, $H_{A'}$, $H_{B'}$, Cym), 3.95 (dm, J = 43.6 Hz, 1H), 3.21 (m, 1H, NCH_2), 2.97, 1.82 (2 × m, 2H, PCH_2), 2.28 (s, 6H, Me *p*-tolyl), 2.22 (sp, 1H, CH iPr), 2.15 (s, 3H, Me Cym), 1.26 (d, J = 6.9 Hz, 3H, Me iPr), 1.20 (d, J = 6.9 Hz, 3H, Me iPr), −8.83 (d, J = 42.9 Hz, 1H, Ru–H). $^{13}C\{^1H\}$ NMR (125.77 MHz, THF-d_8): δ = 156.52 (C═N), 140.52 (d, J = 41.8), 137.77 (d, J = 58.5 Hz), 135.31–129.75 (PPh_2), 139.30, 138.60, 134.65, 133.66, 131.61, 131.29, 120.70, 120.29 (*p*-tolyl), 116.48 (*C*–iPr, Cym), 107.57 (*C*–Me Cym), 92.67 ($CH_{A'}$), 89.36, 88.51 (CH_A, CH_B), 84.76 ($CH_{B'}$), 57.53 (CH_2N), 34.84 (d, J = 30.2 Hz, CH_2P), 33.02 (CH iPr), 24.55, 24.51 (Me iPr), 21.35 (Me *p*-tolyl), 20.27 (Me Cym). $^{31}P\{^1H\}$ NMR (202.46 MHz, THF-d_8. RT): δ = 68.80 (s).

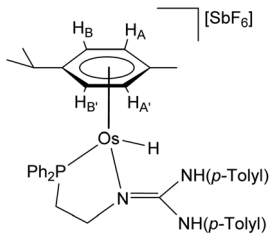

14

Complex 14. HRMS (μ-TOF), $C_{39}H_{45}N_3OsP$, $[M - SbF_6]^+$, calcd: 778.2960, found: 778.2964. ^1H NMR (500.10 MHz, CD_2Cl_2, RT): δ = 7.70–7.24 (m, 10H, PPh_2), 7.19 (s, 1H, NH *trans* CH_2), 7.09, 7.05, 6.87, 6.79 (4 × d, J = 8.0 Hz, 8H, *p*-tolyl), 6.65 (s, 1H, NH *trans* Os), 5.24 (d, J = 6.2 Hz, 1H, H_A), 5.20 (d, 1H, H_B), 4.92 (d, J = 5.9 Hz, 1H, $H_{A'}$), 4.87 (d, 1H, $H_{B'}$), 4.16 (m, J = 43.6 Hz, 1H), 3.15 (m, 1H, NCH_2), 2.99, 1.89 (2 × m, 2H, PCH_2), 2.27, 2.26 (2 × s, 6H, Me *p*-tolyl), 2.25 (sp, 1H, CH iPr), 2.20 (s, 3H, Me Cym), 1.25 (d, J = 6.9 Hz, 3H, Me iPr), 1.22 (d, J = 6.9 Hz, 3H, Me iPr), −9.90 (d, J = 34.6 Hz, 1H, Os–H). $^{13}C\{^1H\}$ NMR (125.77 MHz, CD_2Cl_2): δ = 155.32 (C═N), 138.62 (d, J = 51.1), 135.22 (d, J = 64.3 Hz), 134.95–129.24 (PPh_2), 137.24, 136.15, 135.39, 134.19, 131.27, 130.72, 120.57, 119.80 (*p*-tolyl), 106.57 (*C*–Me Cym), 98.79 (*C*–iPr Cym), 83.81 ($CH_{A'}$), 81.30 (CH_A), 79.70 (CH_B), 74.17 ($CH_{B'}$), 59.52 (CH_2N), 35.38 (d, J = 33.6 Hz, CH_2P), 32.47 (CH iPr), 24.42, 24.26 (Me iPr), 21.26, 21.18 (Me *p*-tolyl), 19.65 (Me Cym). $^{31}P\{^1H\}$ NMR (202.46 MHz, CD_2Cl_2, RT): δ = 29.89 (s).

$^{31}P\{^1H\}$ NMR (202.46 MHz, CD_2Cl_2, 173 K): δ = 30.63 (bs), 30.23 (bs).

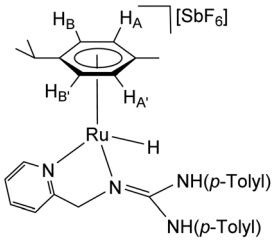

15

Complex 15. HRMS (μ-TOF), $C_{31}H_{37}N_4Ru$, $[M - SbF_6]^+$, calcd: 567.2056, found: 567.2059. ^1H NMR (500.10 MHz, THF-d_8, RT): δ = 8.59 (d, J = 5.7 Hz, 1H, H_6 Py), 8.42 (s, 1H, NH *trans* Ru), 7.79 (t, J = 7.8 Hz, 1H, H_4 Py), 7.34 (d, J = 7.9 Hz, 1H, H_3 Py), 7.28 (t, J = 6.5 Hz, 1H, H_5 Py), 7.14, 7.08 (A parts of an AB system, J(A,B) = 8.0 Hz, 4H, *p*-tolyl), 7.01(s, 1H, NH *trans* CH_2), 6.97 (B parts of an AB system, 4H, *p*-tolyl), 5.63 (d, J = 5.7 Hz, 1H, H_B), 5.50 (d, J = 6.1 Hz, 1H, $H_{A'}$), 5.30 (d, 2H, H_A, $H_{B'}$), 5.25 (d, J = 5.7 Hz, 1H, H_A), 4.85 (AB system, J(A,B) = 18.2 Hz, 2H, CH_2), 2.52 (sp, 1H, CH iPr), 2.29, 2.26 (2 × s, 6H, Me *p*-tolyl), 2.21 (s, 3H, Me Cym), 1.29 (d, J = 6.8 Hz, 3H, Me iPr), 1.26 (d, J = 6.8 Hz, 3H, Me iPr), −5.34 (s, 1H, Ru–H). $^{13}C\{^1H\}$ NMR (125.77 MHz, THF-d_8, RT): δ = 162.73 (CCH_2), 155.25 (CH_6), 138.01 (CH_4), 123.94 (CH_5), 121.13 (CH_3) (Py), 137.95, 137.71, 133.12, 132.10, 130.31, 129.79, 120.06, 119.93 (*p*-tolyl), 110.89 (*C*–iPr Cym), 102.64 (*C*–Me Cym), 84.84 ($CH_{A'}$), 84.56, 80.56 (CH_A, $CH_{B'}$), 83.83 (CH_B), 61.39 (CH_2), 32.42 (CH, iPr), 24.05, 23.23 (Me iPr), 20.51, 20.49 (Me *p*-tolyl), 19.49 (Me Cym).

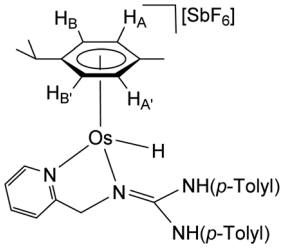

16

Complex 16. HRMS (μ-TOF), $C_{31}H_{37}N_4Os$, $[M - SbF_6]^+$, calcd: 657.2628, found: 657.2631. ^1H NMR (500.10 MHz, THF-d_8, RT): δ = 8.81 (d, J = 5.8 Hz, 1H, H_6 Py), 8.46 (s, 1H, NH *trans* Os), 7.79 (t, J = 7.7 Hz, 1H, H_4 Py), 7.42 (d, J = 7.9 Hz, 1H, H_3 Py), 7.25 (t, J = 6.8 Hz, 1H, H_5 Py), 7.11, 6.95 (AB system, J(A,B) = 8.5 Hz, 4 H, *p*-tolyl), 7.07, 6.96 (AB system, J(A,B) = 8.5 Hz, 4 H, *p*-tolyl), 7.08 (s, 1H, NH *trans* CH_2), 5.71 (d, J = 5.5 Hz, 1H, H_B), 5.59 (d, J = 5.5 Hz, 1H, $H_{A'}$), 5.42 (d, 1H, $H_{B'}$), 5.34 (d, 1 H, H_A), 5.15, 4.78 (AB system, J(A,B) = 18.0 Hz, 2H, CH_2), 2.47 (sp, 1H, CH iPr), 2.31 (s, 3H, Me Cym), 2.28, 2.25 (2 × s, 6H, Me *p*-tolyl), 1.26 (d, J = 7.0 Hz, 3H, Me iPr), 1.24 (d, J = 7.0 Hz, 3H, Me iPr), −5.32 (s, 1H, Os–H). $^{13}C\{^1H\}$ NMR (125.77 MHz, THF-d_8, RT): δ = 163.00 (C═N), 155.5 (CH_6), 153.75 (CCH_2), 138.11 (CH_4), 124.70 (CH_5), 120.79 (CH_3) (Py), 137.88 (CN), 137.68 (CN), 133.37 (*C*Me), 132.36 (*C*Me), 130.38, 129.88, 120.21, 120.04 (*p*-tolyl), 101.11 (*C*–iPr Cym), 94.3 (*C*–Me Cym), 75.99 ($CH_{A'}$), 75.50 (CH_A), 74.77 (CH_B), 71.94 ($CH_{B'}$), 62.76 (CH_2), 32.57 (CH, iPr), 24.23, 23.50 (Me iPr), 20.51, 20.50 (Me *p*-tolyl), 19.58 (Me Cym).

Preparation of orthometalated complexes [(Cym)M(κ³N,N′,C-H_2L3_{-H})][SbF_6] (M = Ru (17), Os (18))

A solution of complex [(Cym)M(κ³N,N′,N″-**HL3**)][SbF_6] (M = Ru (**10**), Os (**11**)) (0.12 mmol) in methanol (5 mL) was heated at 338 K for 8 (Ru) or 30 h (Os). The resulting solution was concentrated under reduced pressure to *ca*. 2 mL. The slow addition of *n*-pentane led to the precipitation of an orange (Ru) or yellow (Os) solid, which was washed with *n*-pentane (3 × 5 mL) and vacuum-dried. Crystals of complex **17** suitable for

X-ray diffraction analysis were obtained by crystallization from methanol/diethyl ether/*n*-pentane solutions.

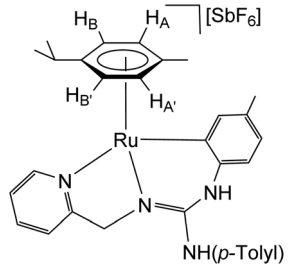

17

Complex 17. Yield: 88.4 mg, 92%. Anal. calcd for $C_{31}H_{35}N_4F_6RuSb$: C, 46.5; H, 4.4; N, 7.0. Found: C, 46.1; H, 4.5; N, 6.7. HRMS (μ-TOF), $C_{31}H_{35}N_4Ru$, $[M - SbF_6]^+$, calcd: 565.1908, found: 565.1930. IR (cm^{-1}): ν(NH) 3386 (br), ν(N═C) 1641 (br), $\nu(SbF_6)$ 655 (s). ^1H NMR (500.10 MHz, CD_3OD, RT): δ = 8.87 (d, J = 5.5 Hz, 1H, H_6 Py), 7.76 (t, J = 7.8 Hz, 1H, H_4 Py), 7.71 (s, 1H, orthometalated *p*-tolyl), 7.34 (t, J = 6.3 Hz, 1H, H_5 Py), 7.27 (1H, H_3 Py), 7.27 (2H, *p*-tolyl), 7.00 (d, J = 8.4 Hz, 2H, *p*-tolyl), 6.69 (bs, 1H), 6.56 (d, 1H, J = 7.8 Hz, orthometalated *p*-tolyl), 5.78 (d, J = 5.8 Hz, 1H, H_B), 5.60 (d, J = 6.0 Hz, 1H, $H_{A'}$), 5.45 (d, 1H, $H_{B'}$), 5.18 (d, 1H, H_A), 4.79 (s, 2H, CH_2), 2.37 (s, 3H, Me *p*-tolyl), 2.31 (s, 3H, Me orthometalated *p*-tolyl), 2.31 (m, 1H, CH iPr), 1.68 (s, 3H, Me Cym), 1.07 (d, J = 6.9 Hz, 3H, Me iPr), 0.95 (d, J = 6.9 Hz, 3H, Me iPr). $^{13}C\{^1H\}$ NMR (125.77 MHz, CD_3OD, RT): δ = 163.09 (CCH_2), 155.75 (CH_6), 139.87 (CH_4), 126.16 (CH_5), 121.75 (CH_3) (Py), 153.97 (C═N), 151.47 (C–Ru), 143.08, 140.44, 134.52, 126.01, 116.68 (orthometalated *p*-tolyl), 139.51, 139.44 (CN), 135.00, 132.11, 121.61 (*p*-tolyl), 111.28 (*C*–iPr Cym), 101.65 (*C*–Me Cym), 91.86 ($CH_{A'}$), 91.06 (CH_B), 84.71 ($CH_{B'}$), 83.65 (CH_A), 64.87 (CH_2), 33.08 (CH iPr), 23.82, 23.15 (Me iPr), 21.80, 21.65 (Me *p*-tolyl), 19.00 (Me Cym).

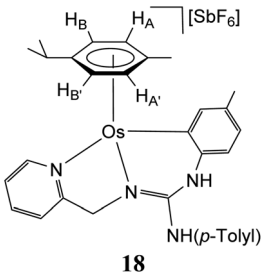

18

Complex 18. Yield: 90.3 mg, 86%. Anal. calcd for $C_{31}H_{35}N_4F_6OsSb$: C, 41.85; H, 4.0; N, 6.3. Found: C, 42.1; H, 4.0; N, 6.0. HRMS (μ-TOF), $C_{31}H_{35}N_4Os$, $[M - SbF_6]^+$, calcd: 655.2472, found: 655.2500. IR (cm^{-1}): ν(NH) 3383 (br), ν(N═C) 1635 (m), $\nu(SbF_6)$ 655 (s). ^1H NMR (500.10 MHz, CD_3OD, RT): δ = 8.96 (d, J = 5.6 Hz, 1H, H_6 Py), 7.76 (t, J = 7.8 Hz, 1H, H_4 Py), 7.59 (s, 1H, orthometalated *p*-tolyl), 7.34 (t, J = 8.4 Hz, 1H, H_5 Py), 7.31 (d, 1H, H_3 Py), 7.27, 7.00 (2 × d, J = 8.4 Hz, 4H, *p*-tolyl), 6.63, 6.57 (2 × d, J = 7.9 Hz, 2H, orthometalated *p*-tolyl), 5.73 (d, J = 5.3 Hz, 1H, H_B), 5.67 (d, J = 5.5 Hz, 1H, $H_{B'}$), 5.59 (d, 1H, $H_{A'}$), 5.44 (d, 1H, H_A), 5.12 (d, J = 16.2 1H), 4.66 (d, 1H) (CH_2), 2.37, 2.26 (2 × s, 6H, Me *p*-tolyl), 2.26 (m, 1H, CH iPr), 1.79 (s, 3H, Me Cym), 1.08 (d, J = 6.9 Hz, 3H, Me iPr), 0.95 (d, J = 6.9 Hz, 3H, Me iPr). $^{13}C\{^1H\}$ NMR (125.77 MHz, CD_3OD, RT): δ = 162.59 (CCH_2), 155.23 (CH_6), 140.09 (CH_4), 126.65 (CH_3), 121.52 (CH_5) (Py), 153.39 (C═N), 143.06, 140.26 (C–Os), 139.79, 135.05, 126.18, 116.23 (orthometalated *p*-tolyl), 139.41, 139.33 (CN), 135.19, 132.12, 121.76 (*p*-tolyl), 101.04 (*C*–iPr Cym), 93.49 (*C*–Me Cym), 81.42, 81.38 (CH_B, $CH_{A'}$), 76.18 ($CH_{B'}$), 74.90 (CH_A), 66.39 (CH_2), 33.14 (CH iPr), 23.96, 23.64 (Me iPr), 21.67, 21.64 (Me *p*-tolyl), 18.92 (Me Cym).

Preparation of [(Cym)Ru(κ^{3}N,N′,C-H_2L3$_{-H}$)(CH_2CHCOOMe)][SbF_6] (19)

A high-pressure NMR tube containing complex **9** (13.3 mg, 0.015 mmol) and methyl acrylate (27.2 μL, 0.30 mmol) in THF-d_8 (0.45 mL) was pressurised with hydrogen gas (5 bar). The tube was heated for 10 h at 90 °C and the resulting solution was vacuum-evaporated to dryness. The slow addition of diethyl ether led to the precipitation of a brown solid which was washed with diethyl ether (3 × 1 mL) and vacuum-dried. Crystals of **19** suitable for X-ray diffraction analysis were obtained by crystallisation from THF-d_8 solutions. This compound was also prepared working under similar conditions but in the absence of hydrogen.

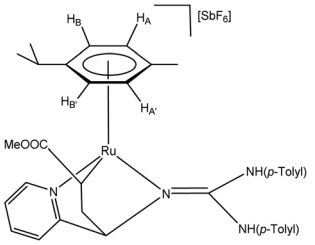

19

Complex 19. Yield: 11.9 mg, 90%. Anal. calcd for $C_{35}H_{41}N_4O_2F_6RuSb$·THF: C, 48.9; H, 5.1; N, 5.8. Found: C, 48.9; H, 5.0; N, 5.9. HRMS (μ-TOF), $C_{35}H_{41}N_4O_2Ru$, $[M]^+$, calcd: 651.2268, found: 651.2259. IR (cm^{-1}): ν(NH) 3401 (br), ν(C═O) 1721, ν(C═N) 1655, $\nu(SbF_6)$ 655 (s).

$R_{Ru}R_{C(16)}R_{C(32)}$-**19**. ^1H NMR (500.10 MHz, CD_2Cl_2, RT): δ = 8.83 (d, J = 5.8 Hz, 1H, H_6 Py), 7.72 (t, J = 7.6 Hz, 1H, H_4 Py), 7.32 (t, J = 5.9 Hz, 1H, H_5 Py), 6.82 (1H, H_3 Py), 7.14–6.79 (m, 8 H, *p*-tolyl), 5.30 (d, J = 6.1 Hz, 1H, H_B), 5.26 (d, J = 6.1 Hz, 1H, $H_{A'}$), 5.13 (d, 1H, $H_{B'}$), 4.97 (d, 1H, H_A), 4.70 (d, J = 5.5 Hz, 1H, C*HN), 3.88 (s, 3H, OMe), 2.92 (sp, 1H, CH iPr), 2.42 (d, J = 9.4 Hz, 1H, C*HRu), 2.31 (s, 6H, Me *p*-tolyl), 2.30 (s, 3H, Me Cym), 1.96, 1.22 (2 × m, 2H, CH_2), 1.26, 1.19 (2 × d, J = 6.8 Hz, 6H, Me iPr). $^{13}C\{^1H\}$ NMR (125.77 MHz, CD_2Cl_2, RT): δ = 188.31 (C═O), 164.22 (N*C*) (Py), 155.22 (C═N), 153.36(CH_6), 139.37 (CH_4), 124.20 (CH_5), 121.11 (CH_3) (Py), 135.76, 131.38, 120.86, 120.61 (*p*-tolyl), 106.94 (*C*–iPr Cym), 99.46 (*C*–Me Cym), 88.51 (CH_B), 88.22 ($CH_{A'}$), 83.73 (CH_A), 83.18 ($CH_{B'}$), 70.54 (C*N), 50.95 (OMe), 36.87 (CH_2), 31.03 (CH, iPr), 26.16 (C*Ru), 23.84, 21.31 (Me iPr), 21.31 (Me *p*-tolyl), 18.96 (Me Cym).

$R_{Ru}R_{C(16)}S_{C(32)}$-**19**. ^1H NMR (500.10 MHz, CD_2Cl_2, RT): δ = 8.47 (d, J = 5.6 Hz, 1H, H_6 Py), 8.33, 7.38 (2 × s, 2H, NH), 7.66

(t, J = 7.6 Hz, 1H, H_4 Py), 7.26 (t, J = 5.9 Hz, 1H, H_5 Py), 6.82 (1H, H_3 Py), 7.18–6.65 (m, 8 H, *p*-tolyl), 5.69 (d, J = 5.7 Hz, 1H, H_B), 5.13 (d, J = 6.0 Hz, 1H, $H_{A'}$), 5.09 (d, 1H, $H_{B'}$), 4.70 (d, 1H, H_A), 4.86 (bd, J = 3.9 Hz, 1H, C*HN), 3.98 (d, J = 6.0 Hz, 1H, C*HRu), 3.21 (s, 3H, OMe), 2.84 (sp, 1H, CH *i*Pr), 2.40 (s, 3H, Me Cym), 2.25 (s, 6H, Me *p*-tolyl), 1.69 (m, 1H), 1.45 (bd, J = 13.1 Hz, 1H) (CH_2), 1.25, 1.21 (2 × d, J = 6.9 Hz, 6H, Me iPr). $^{13}C\{^1H\}$ NMR (125.77 MHz, CD_2Cl_2, RT): δ = 182.11 (C═O), 163.97 (NCC*) (Py), 154.47 (C═N), 152.43 (CH_6), 138.56 (CH_4), 124.37 (CH_5), 120.98 (CH_3) (Py), 135.93, 130.92, 122.12, 120.98 (*p*-tolyl), 107.61 (*C*–iPr Cym), 103.43 (*C*–Me Cym), 87.55 (CH_B), 84.94 ($CH_{A'}$), 84.34 ($CH_{B'}$), 77.79 (CH_A), 71.02 (C*N), 51.30 (OMe), 35.01 (CH_2), 31.50 (CH, iPr), 27.69 (C*Ru), 23.84, 23.53 (Me iPr), 21.31 (Me *p*-tolyl), 18.89 (Me Cym).

General procedure for the catalytic hydrogenation reactions

A high-pressure NMR tube containing the catalyst (0.015 mmol) and the substrate to be hydrogenated (0.30 mmol) in THF-d_8 (0.45 mL) was pressurised with hydrogen gas (5 bar). The tube was heated at the appropriate temperature and the solution was monitored by NMR. Conversion values were determined by ^{1}H NMR.

Author contributions

S.B. and A.G.: synthetic and catalytic work. F.V. and R.R.: characterization and supervision of the work. P.G. and F.J.L.: crystallographic analysis. J.A.L.: DFT calculations. P.L. and D. C.: design and supervision of the work. P.G., F.J.L., J.A.L., P.L. and D.C.: writing of the manuscript. All authors have given their approval to the final version of the manuscript.

Conflicts of interest

The authors declare that they have no known competing financial interests or personal relationships that could have appeared to influence the work reported in this paper.

Acknowledgements

We thank the Ministerio de Economía y Competitividad of Spain (PID2021-122406NB-100, PID2020-119512GB-I00 and CTQ2018-095561-BI00) and Gobierno de Aragón (Grupo de Referencia: Catálisis Homogénea Enantioselectiva, E05_20R and E05_23R) for financial support. Amie Parker is acknowledged for experimental assistance.

References

1 G. C. Wel, R. R. San Juan, J. D. Masuda and D. W. Stephan, *Science*, 2006, **314**, 1124–1126.

2 (*a*) *Molecular Catalysis, Frustrated Lewis Pairs Vol. 2*, ed. J. C. Slootweg and A. R. Jupp, Springer, Switzerland, 2021; (*b*) A. R. Jupp and D. W. Stephan, *Trends Chem.*, 2019, **1**, 35–48; (*c*) J. Paradies, *Coord. Chem. Rev.*, 2019, **380**, 170–183; (*d*) D. J. Scott, M. J. Fuchter and A. E. Ashley, *Chem. Soc. Rev.*, 2017, **46**, 5689–5700; (*e*) D. W. Stephan, *Science*, 2016, **354**, aaf7229; (*f*) D. W. Stephan, *J. Am. Chem. Soc.*, 2015, **137**, 10018–10032; (*g*) D. W. Stephan and G. Erker, *Angew. Chem., Int. Ed.*, 2015, **54**, 6400–6441; (*h*) D. W. Stephan, *Acc. Chem. Res.*, 2015, **48**, 306–316; (*i*) *Topics in Current Chemistry, Frustrated Lewis Pairs II: Expanding the Scope*, ed. G. Erker and D. W. Stephan, Springer, Heidelberg, 2013, vol. 334; (*j*) *Topics in Current Chemistry, Frustrated Lewis Pairs I: Uncovering and Understanding*, ed. G. Erker and D. W. Stephan, Springer, Heidelberg, 2013, vol. 332; (*k*) D. W. Stephan and G. Erker, *Angew. Chem., Int. Ed.*, 2010, **49**, 46–76.

3 (*a*) S. R. Flynn and D. F. Wass, *ACS Catal.*, 2013, **3**, 2574–2581; (*b*) H. B. Hamilton, A. M. King, H. A. Sparkes, N. E. Pridmore and D. F. Wass, *Inorg. Chem.*, 2019, **58**, 6399–6409; (*c*) A. M. Chapman, M. F. Haddow and D. F. Wass, *J. Am. Chem. Soc.*, 2011, **133**, 8826–8829; (*d*) Z. Jian, C. G. Daniliuc, G. Kehra and G. Erker, *Organometallics*, 2017, **36**, 424–434; (*e*) A. T. Normand, C. G. Daniliuc, B. Wibbeling, G. Keh, P. Le Gendre and G. Erker, *J. Am. Chem. Soc.*, 2015, **137**, 10796–10808; (*f*) X. Xu, G. Kehr, C. G. Daniliuc and G. Erker, *J. Am. Chem. Soc.*, 2013, **135**, 6465–6476; (*g*) S. Zhang, A. M. Appel and R. M. Bullock, *J. Am. Chem. Soc.*, 2017, **139**, 7376–7387; (*h*) B. R. Barnett, M. L. Neville, C. E. Moore, A. L. Rheingold and J. S. Figueroa, *Angew. Chem., Int. Ed.*, 2017, **56**, 7195–7199; (*i*) S. Zhang, A. M. Appel and M. Bullock, *J. Am. Chem. Soc.*, 2017, **139**, 7376–7387.

4 (*a*) T. C. Johnstone, G. N. J. H. Wee and D. W. Stephan, *Angew. Chem., Int. Ed.*, 2018, **57**, 5881–5884; (*b*) S. Roters, C. Appelt, H. Westenberg, A. Hepp, J. C. Slootweg, K. Lammertsma and W. Uhl, *Dalton Trans.*, 2012, **41**, 9033–9045; (*c*) M. Boudjelel, E. D. S. Carrizo, S. Mallet-Ladeira, S. Massou, K. Miqueu, G. Bouhadir and D. Bourissou, *ACS Catal.*, 2018, **8**, 4459–4464; (*d*) M. J. Sgro and D. W. Stephan, *Angew. Chem Int. Ed.*, 2012, **51**, 11343–11345.

5 (*a*) M. Carmona, J. Ferrer, R. Rodríguez, V. Passarelli, F. J. Lahoz, P. García-Orduña, L. Cañadillas-Delgado and D. Carmona, *Chem. – Eur. J.*, 2019, **25**, 13665–13670; (*b*) A. Parker, P. Lamata, F. Viguri, R. Rodríguez, J. A. López, F. J. Lahoz, P. García-Orduña and D. Carmona, *Dalton Trans.*, 2020, **49**, 13601–13617; (*c*) E. T. Wilkinson, F. Viguri, R. Rodríguez, J. A. López, F. J. Lahoz, P. García-Orduña, P. Lamata and D. Carmona, *Helv. Chim. Acta*, 2021, **104**, e2100044; (*d*) M. Carmona, R. Pérez, J. Ferrer, R. Rodríguez, V. Passarelli, F. J. Lahoz, P. García-Orduña and D. Carmona, *Inorg. Chem.*, 2022, **61**, 13149–13164.

6 (*a*) M. A. Bennet, T. N. Huang, T. W. Matheson and A. K. Smith, *Inorg. Synth.*, 1982, **21**, 75; (*b*) J. Cabeza and P. M. Maitlis, *J. Chem. Soc., Dalton Trans.*, 1985, 573–578.

7 The ligand **H_2L1** was prepared *in situ* from 2-(1-diphenylphosphano)ethylamine and *p*-tolylisothiocyanate following literature procedures: (*a*) H.-P. Deng and M. Shi, *Eur. J. Org. Chem.*, 2012, 183–187; (*b*) Y.-L. Yang, C.-K. Pei and M. Shi,

Org. Biomol. Chem., 2011, **9**, 3349–3358; (*c*) H.-P. Deng, Y. Wei and M. Shi, *Eur. J. Org. Chem.*, 2011, 1956–1960; (*d*) Y.-L. Shi and M. Shi, *Adv. Synth. Catal.*, 2007, **349**, 2129–2135.

8 Compounds **5** and **6** are fluxional in solution. From $^{31}P\{^{1}H\}$ NMR measurements, an activation energy at the coalescence temperature of 9.50 ± 0.12 and 8.89 ± 0.12 Kcal mol^{-1} for **5** and **6**, respectively, has been calculated. DFT calculations reveal that these experimental values can be accounted for by assuming that the dynamic behaviour consist of rotation around the arene centroid-metal axis and about the SC–N(*p*-Tolyl) bond. For details see ESI.† .

9 (*a*) R. S. Cahn, C. Ingold and V. Prelog, *Angew. Chem., Int. Ed. Engl.*, 1966, **5**, 385–415; (*b*) V. Prelog and G. Helmchen, *Angew. Chem., Int. Ed. Engl.*, 1982, **21**, 567–583; (*c*) C. Lecomte, Y. Dusausoy, J. Protas, J. Tirouflet and A. Dormond, *J. Organomet. Chem.*, 1974, **73**, 67–76.

10 Compounds **11** and **12** are fluxional in solution. From $^{31}P\{^{1}H\}$ NMR measurements, an activation energy at the coalescence temperature of 10.18 ± 0.12 and 10.02 ± 0.12 Kcal mol^{-1} for **11** and **12**, respectively, has been calculated. DFT calculations do not conclusively discriminate between a dynamic behaviour consisting of rotation around the arene centroid-metal axis and about the SC–N (*p*-tolyl) bond (as for complexes **5** and **6**) or an exchange between two conformations within the seven-membered metalacycle involving the phosphano-thiourea ligand. For details see ESI.†

11 (*a*) *Topics in Current Chemistry, Frustrated Lewis Pairs I: Uncovering and Understanding*, ed. G. Erker and D. W. Stephan, Springer, Heidelberg, 2013, vol. 332, p 157–212; (*b*) J. Paradies, *Eur. J. Org. Chem.*, 2019, 283–294; (*c*) N. Hidalgo, J. J. Moreno, M. Pérez-Jiménez, C. Maya, J. López-Serrano and J. Campos, *Chem. – Eur. J.*, 2020, **26**, 5982–5993.

12 (*a*) J. W. Kang and P. M. Maitlis, *J. Organomet. Chem.*, 1971, **30**, 127–133; (*b*) G. Ciancaleoni, S. Bolaño, J. Bravo, M. Peruzzini, L. Gonsalvi and A. Macchioni, *Dalton Trans.*, 2010, **39**, 3366–3368; (*c*) S. Banerjee, J. J. Soldevila-Barreda, J. A. Wolny, C. A. Wootton, A. Habtemariam, I. Romero-Canelón, F. Chen, G. J. Clarkson, I. Prokes, L. Song, B. Peter, P. B. O'Connor, V. Schünemann and P. J. Sadler, *Chem. Sci.*, 2018, **9**, 3177–3185; (*d*) A. Sink, S. Banerjee, J. A. Wolny, C. Imberti, E. C. Lant, M. Walker, V. Schünemann and P. J. Sadler, *Dalton Trans.*, 2022, **51**, 16070–16081; (*e*) C. Ferrer, J. Ferrer, V. Passarelli, F. J. Lahoz, P. García-Orduña and D. Carmona, *Organometallics*, 2022, **41**, 1445–1453.

13 Date of search: 20-07-2023. Version: 2022.3.0. C. R. Groom, I. J. Bruno, M. P. Lightfoot and S. C. Ward, *Acta Crystallogr., Sect. B: Struct. Sci., Cryst. Eng. Mater.*, 2016, **72**, 171–179.

14 C. Gunanathan and D. Milstein, *Acc. Chem. Res.*, 2011, **44**, 588–602.

15 E. L. Eliel, S. H. Wilen and L. H. Mander, *Stereochemistry of Organic Compounds*, Wiley-Interscience, New York, 1994, p. 159.